J-Researchers

Journal of Civil Engineering Researchers

Journal homepage: www.journals-researchers.com

Investigation of Seismic Behavior in Steel Frames Equipped with Semi-Active Rotational Friction Dampers

Hadi Bahri [a]

[a] Department of Civil Engineering, Cha.C., Islamic Azad University, Chalus, Iran

ABSTRACT

This study examines the performance of semi-active friction dampers in reducing structural responses during near-field earthquakes, specifically Chi-Chi, Kobe, Tabas, and Gazli. These dampers feature two sliding plates where the contact force is dynamically adjusted via a control algorithm to optimize the force on the structure. We applied the Linear Quadratic Regulator (LQR) algorithm and clipping control law to compute this force in real time. A ten-story steel frame with X-shaped bracing was modeled in ETABS to derive mass and stiffness matrices, then time-history dynamic analysis was performed in MATLAB under the selected earthquakes, which vary in frequency content. Responses were compared across passive, active, and semi-active modes, as well as four damper layouts. Findings show that semi-active control reduces displacements more effectively than other modes. Placing dampers around the plan perimeter offers the best results; for example, under Chi-Chi, base shear rose by 41.4% in active mode and 84.86% in passive mode compared to semi-active.

ARTICLE INFO

Received: August 18,2025
Accepted: November 06,2025

Keywords:
Friction damper
semi-active control
seismic behavior of steel frames
dynamic analysis

DOI: 10.61186/JCER.8.1.61
DOR: 20.1001.1.22516530.1399.11.4.1.1

Introduction

Earthquakes have historically caused significant structural damage and loss of life, necessitating advanced design strategies to enhance seismic resilience [1]. Building codes have been developed to ensure structures can withstand lateral loads, with a primary design objective of enabling structures to resist internal forces induced by seismic events [1]. However, standalone structures often lack the capacity to endure severe seismic excitations, highlighting the need for innovative vibration control systems [2]. These systems are categorized into three primary types: passive, active, and semi-active control [2]. Semi-active control systems combine the high reliability of passive systems with the adaptability of active systems, requiring only minimal electrical energy—comparable to that of a battery—making them particularly advantageous during severe earthquakes when external power sources may be disrupted [6, 9]. Such systems incorporate devices capable of dynamically adjusting stiffness or damping parameters, with semi-active friction dampers demonstrating significant efficacy in mitigating structural vibrations [6].

The concept of seismic control was first introduced in the 1950s by Kobori and Minai, who emphasized the importance of controlling a structure's seismic response due to the unpredictable nature of ground vibrations [4]. By 1972, Yao proposed a comprehensive control theory grounded in structural control principles, introducing an adaptive system designed to address stability challenges by responding to unpredictable loading and environmental conditions, ensuring optimal performance across all loading scenarios [15]. In the early 1980s, Pall and Marsh developed passive friction dampers, evaluating their performance in ten-story steel frames with moment-resisting (MR), buckling-restrained braced (BRB), and friction-damped braced (FBD) configurations. Their findings indicated that FBDs, utilizing sliding loads,

provided lateral resistance equivalent to approximately 90 kips per floor for MR frames, with top-floor deformations reduced by 40% compared to MR frames and 50% compared to BRB frames [11]. Mualla (2000) conducted experimental tests on friction dampers at displacement amplitudes of 5, 10, 15, and 20 mm and a frequency of 0.3 Hz, demonstrating consistent friction force despite increasing displacements [7]. Liao et al. (2004) tested a three-story steel frame equipped with friction dampers on a shaking table under the El Centro, Kobe, and Chi-Chi earthquakes, revealing reduced damage to joints, frame members, and connections, as well as decreased vibrations [5]. Fisco and Adeli (2011) reviewed active and semi-active damper systems, noting that tuned mass dampers (TMDs) perform effectively against earthquake-induced vibrations but are less efficient against wind-induced vibrations [2]. Nazari Monfared and Zohraei (2016) investigated seismic control in multi-story buildings using active tendons and soil-structure interaction, identifying the Linear Quadratic Regulator (LQR) algorithm as optimal for reducing displacement in the x-direction [8]. Lu et al. (2018) demonstrated that semi-active friction dampers enhance structural performance and reduce displacements during seismic events [6]. Ghanadi Asl et al. (2022) evaluated out-of-plane braced frame systems with optimized rotary friction dampers, showing improved seismic responses across various seismic intensity levels [3].

This study investigates the performance of semi-active friction dampers in controlling vibrations in steel frames. A ten-story steel structural model was selected, and the equations of motion for the system equipped with friction dampers were formulated under seismic excitations. A MATLAB-based program was developed to solve these equations and perform time-history dynamic analysis, enabling a comprehensive evaluation of the dampers' effectiveness in enhancing seismic performance.

2.Research Methodology

This study investigates the effectiveness of semi-active friction dampers in controlling steel frame vibrations. A structural model was selected, and equations of motion for the system with friction dampers were formulated under earthquake vibrations. A MATLAB program was developed for time-history dynamic analysis.

2.1.Friction Damper

Friction dampers convert seismic energy into heat reliably and economically. A normal contact force compresses two sliding plates. In passive friction dampers, this force is constant, while in semi-active dampers, it is controllable, derived as follows :

$$N(t) = N_{pre} + C_{pz}V(t) \quad (1)$$

Where N is the total normal contact force; Npre is the pre-load of the damper; Cpz is the piezoelectric actuator coefficient; and VV is the applied voltage. The frictional force generated by the semi-active damper is denoted by f and is expressed as relationship .

$$f(t) = \mu N(t) sgn\,(\dot{x}) if \dot{x} \neq 0 \quad (2)$$

$$-\mu N(t) \leq f(t) \leq \mu N(t) if \dot{x} = 0$$

Where μ is the friction coefficient of the damper, and sgn(ẋ) indicates the direction of damper slip. During structural movement, the friction damper operates in two phases: a sticking phase and a slipping phase. In the slipping phase, the slip velocity is non-zero, and the friction force is calculated from the first line of Equation (2). In the sticking phase, the two friction plates adhere to each other, and the slip velocity is zero. The positive value of the friction force in the sticking phase can be approximated by Equation.

$$f\_s = |f\_i + f\_r\,| when |f| \geq f\_s\ and \dot{x} = 0 \quad (3)$$

Where fi is the inertia force applied to the mass, and fr is the restoring force provided by the stiffness of the structure.

2.2- LQR Control Algorithm

In designing an optimal system, the goal is to minimize the maximum structural responses with minimal energy or control force input to the system. The optimal control algorithm, known as LQR (Linear Quadratic Regulator), determines the control force by minimizing the standard second-order performance index according to relationship.

$$J = \frac{1}{2}\int_{t_0}^{t_f} (Z'QZ + F_c'RF_c + 2 \times Z'NF_c)\, dt \quad (4)$$

In the above relationship, the parameters t_0 and tf represent the start and end times of the applied control force, respectively. The control force is denoted by Fc. The matrices Q, R, and N are weighting matrices, where it is commonly assumed that matrix N is equal to zero in civil engineering discussions and structural system analyses. With this assumption, the above relationship transforms into relationship *Discretization Techniques for Motion Equations.*

$$J = \frac{1}{2}\int_{t_0}^{t_f} (Z'QZ + F_c'RF_c)\, dt \quad (5)$$

The weighting matrices Q and R represent the relative importance of state variables and control forces in the minimization process. Assigning larger values to the elements of Q indicates a greater emphasis on reducing control responses, while assigning larger values to R reflects the aim to use less energy due to the complexity of existing economic or capacity constraints.

In this paper, since the control system is installed on each floor, the weighting matrices R and Q are considered as relationships (6) and (7) respectively[11].

$$Q = 1000 \times I_{2n\times 2n} \quad (6)$$

$$R = 0.01 \times I_{n\times n} \quad (7)$$

Where M and K are the mass and stiffness matrices of the structure, and II is the identity matrix, with n being the number of floors in the structure. Using the LQR control algorithm, the vector of control forces is determined at each moment.

In the friction damper, the contact force between the damper plates must be adjusted at each moment to exert a force similar to the active control force on the structure. The friction damper can only provide a resisting force to the structure when its force direction is opposite to the direction of the sliding velocity of the damper. Furthermore, the friction damper is only capable of exerting control force during the sliding phase. Therefore, the semi-active control force is defined based on the shear control law as relationship [12].

$$N(t) = \begin{cases} \frac{F_{active}}{\mu} if F_{active} \times \dot{u} < 0 \\ 0 if F_{active} \times \dot{u} \geq 0 \end{cases} \quad (8)$$

Where Factive is the active control force calculated by the LQR algorithm, and μ is the coefficient of friction of the friction damper.

2.3Equations of Motion for a Structure Equipped with Semi-Active Friction Dampers

For an n-story shear frame subjected to base acceleration $\ddot{x}_g$, the equation of motion for this structure, equipped with semi-active friction dampers on all stories, is expressed by Equation.

$$M\ddot{X}(t) + C\dot{X}(t) + KX(t) + Me\ddot{x}_g + Df_{SA}(t) \quad (9)$$

In this relation, t denotes time. The vectors X(x_1, x_2, ..., x_n), $\dot{X}$($\dot{x}_1$, $\dot{x}_2$, ..., $\dot{x}_n$), and $\ddot{X}$($\ddot{x}_1$, $\ddot{x}_2$, ..., $\ddot{x}_n$) represent the displacement, velocity, and acceleration vectors, respectively. The vector $e^T = [-1, -1, ..., -1]_{1xn}$ is the base acceleration transfer vector. Furthermore, f_{sa} is the control force vector generated by the friction dampers. The mass, damping, stiffness, and friction damper location matrices are calculated according to equation (10).

The mass, damping, stiffness matrices, and the installation locations of the friction dampers are calculated as relationship .

$$M = \begin{bmatrix} m_1 & 0 & \cdots & 0 \\ 0 & m_2 & \cdots & 0 \\ \vdots & \vdots & \ddots & \vdots \\ 0 & 0 & \cdots & m_n \end{bmatrix}_{n\times n} \quad (10)$$

$$C = \begin{bmatrix} c_1 + c_2 & -c_2 & \cdots & 0 \\ -c_2 & c_2 + c_3 & \cdots & 0 \\ \vdots & \vdots & \ddots & \vdots \\ 0 & 0 & \cdots & c_n \end{bmatrix}_{n\times n}$$

$$K = \begin{bmatrix} k_1 + k_2 & -k_2 & \cdots & 0 \\ -k_2 & k_2 + k_3 & \cdots & 0 \\ \vdots & \vdots & \ddots & \vdots \\ 0 & 0 & \cdots & k_n \end{bmatrix}_{n\times n}$$

$$D = \begin{bmatrix} 1 & -1 & 0 & \cdots & 0 \\ 0 & 1 & -1 & \cdots & 0 \\ 0 & 0 & 1 & \cdots & \vdots \\ \vdots & \vdots & \vdots & \ddots & -1 \\ 0 & 0 & 0 & \cdots & 1 \end{bmatrix}_{n\times n}$$

The equations of motion for the structure can be written in state space form as shown in relationship.

$$\dot{Z}(t) = AZ(t) + Bf_{SA}(t) + E\ddot{x}_g(t)) \quad (11)$$

Z is the state vector of the system as shown in relationship (15), and A is the system matrix, B is the matrix applying the control force, and E is the matrix applying the earthquake force, which are presented respectively in relationships (12) to (15)

$$Z(t) = \begin{bmatrix} X(t) \\ \dot{X}(t) \end{bmatrix} \quad (12)$$

$$A = \begin{bmatrix} [0] & [I] \\ -M^{-1}K & -M^{-1}C \end{bmatrix}_{2n\times 2n} \quad (13)$$

$$B = \begin{bmatrix} [0] \\ M^{-1}D \end{bmatrix}_{2n\times n} \quad (14)$$

$$E = \begin{bmatrix} [0] \\ e \end{bmatrix}_{2n\times 1} \quad (15)$$

The equation of motion for the structure is solved step-by-step using the Runge-Kutta method in the MATLAB environment.

Equations of Motion for the Structure Equipped with Passive Friction DamperThe equation of motion for a system with nn degrees of freedom in a general matrix form is represented by relationship.

$$M\ddot{U}(t) + C\dot{U}(t) + kU(t) = Ef \quad (16)$$

By defining the structural system based on the state-space form for the system's equation of motion, in the case where $\dot{x}_0 = 0$, relation (17) is obtained .

$$\dot{\ddot{X}} = AX + B\hat{U} \quad (17)$$

In this case, the matrices A and B and the state vector of the system are given according to relationship .

$$\dot{X} = \begin{Bmatrix} U \\ \dot{U} \end{Bmatrix}_{2n*1} \quad (18)$$

$$A = \begin{bmatrix} O & I \\ -\frac{K}{M} & -\frac{C}{M} \end{bmatrix}_{2n*2n}$$

$$B = \begin{bmatrix} O \\ I \end{bmatrix}_{2n*n}$$

3.In the above relation, the vector Ẋ is the state vector of the system, Û is the system's input vector, and f is the external excitation vector of the system. Matrix A represents the dynamic characteristics of the system, matrix B represents the system input, and matrix E represents the external excitation. Furthermore, in matrix A, the matrices I and 0 denote the identity and zero matrices of size n×n, respectively Dynamic Response Calculation of Soil Systems.

2.4 Equations of Motion for the Structure Equipped with Active Friction Damper

The equation of motion for a system with n degrees of freedom is represented in a general matrix form as shown in relationship.

$$M\ddot{U}(t) + C\dot{U}(t) + kU(t) = Ef + act\hat{U} \quad (19)$$

By describing the structural system based on the state-space form, we have the following equation for the system's motion.

$$\dot{X} = AX(t) + B\hat{U}(t) + EQf(t) \quad (20)$$

In this case, the matrices A and B and the state vector of the system are determined according to relationship

$$M\ddot{U}(t) + C\dot{U}(t) + kU(t) = Ef + act\hat{U} \quad (19)$$

By describing the structural system based on the state-space form, we have the following equation for the system's motion.

$$\dot{X} = AX(t) + B\hat{U}(t) + EQf(t) \quad (20)$$

In this case, the matrices A and B and the state vector of the system are determined according to relationship .

$$\dot{X} = \begin{Bmatrix} U \\ \dot{U} \end{Bmatrix}_{2n*1}$$

$$A = \begin{bmatrix} O & I \\ -\frac{K}{M} & -\frac{C}{M} \end{bmatrix}_{2n*2n} \quad (21)$$

$$B = \begin{bmatrix} O \\ \frac{D}{M} \end{bmatrix}_{2n*n} \quad EQ = \begin{bmatrix} O \\ \frac{E}{M} \end{bmatrix}_{2n*n} \quad D = \begin{bmatrix} D_1 & 0 & 0 \\ 0 & \ddots & 0 \\ 0 & 0 & D_n \end{bmatrix}$$

Matrix D indicates the placement of the actuators.

2.5 -Least Squares Error

The least squares error is a statistical measure of the magnitude of a varying quantity, which is obtained according to relationship (22). This statistical method is used to determine the amount of error present in calculations and in solving equation.

$$x_{rms} = \sqrt{\frac{x_1^2 + x_2^2 + \cdots + x_n^2}{n}} \quad (22)$$

x corresponds to the relevant variable for error determination, and xrms represents the magnitude of the error.

3. Validation

Figure 1: Five-story shear frame equipped with a base isolation system illustrates the structure under consideration, with a semi-active friction damper placed between the foundation and the ground. The performance was evaluated in both passive and semi-active control modes. Structural responses, including maximum base displacement, inter-story drift, and acceleration, were compared (Table 1). Ozbulut et al. (2011) used the LQG algorithm, while this study employed the LQR algorithm, with negligible differences confirming the accuracy of the dynamic analysis. Figure 2 shows the time history of base displacement under the El Centro earthquake, with all labels in English, achieving satisfactory accuracy.

Base Isolation System:This system is used to protect structures against earthquakes. Its fundamental operation involves placing the structure on bearings or elastomeric isolators (such as lead-rubber bearings). These isolators act like a filter, absorbing a significant portion of the ground's vibrational energy and preventing it from being transmitted to the structure. As a result, the structure undergoes a smooth and uniform motion during an earthquake, rather than a sharp and hazardous one.

3.1 Vibration and Oscillation in Testing

To evaluate the performance of this base isolation system in a laboratory environment, earthquake conditions must be simulated. This is typically done using a "Shaking Table." A shaking table is a platform that can oscillate withvarious motion patterns (simulating earthquakes) in a controlled manner, upon which the structural model under testing is placed.

3.2 The Role of the VFD (Variable Frequency Drive

To precisely control the speed and torque of the electric motors that drive this shaking table, a Variable Frequency Drive (VFD) is used. By altering the frequency and voltage supplied to the electric motor, the VFD accurately controls its rotational speed. This precise control enables the shaking table to:

Generate various accelerations and frequencies (simulating different types of earthquakes).

Execute complex motion patterns (such as real earthquake records) with high accuracy.

Start and stop motion in a fully controlled manner.

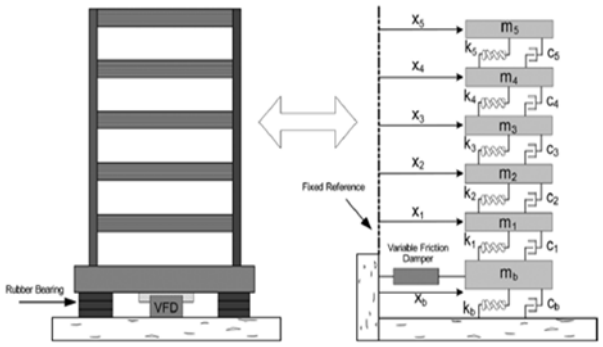

Figure 1: Five-story shear frame equipped with a base isolation system

his paper investigated the effectiveness of two adaptive control strategies for modulating the control force of variable friction dampers (VFDs), which are used as semi-active devices in combination with multilayer rubber bearings for seismic protection of buildings. Their results show that the developed adaptive controllers can successfully improve the seismic response of foundation-isolated buildings to different types of earthquakes.

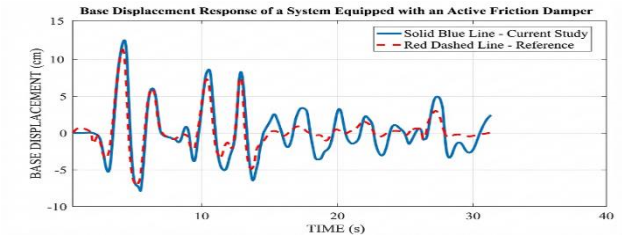

Figure 2: Base displacement with semi-active friction damper during the El Centro earthquake (this study).

Table 1:
Responses of Structures Based on the Conducted Study and Current Study (Validation)

EQ	Resp	Conducted Study			Present Study		
		UC	P	SA	UC	P	SA
El Centro	$x_{b,max}$	20.37	4.95	10.45	19.96	5.22	12.83
	$d_{s,max}$	0.12	0.12	0.09	0.11	0.11	0.08
	$\ddot{x}2_{s,max}$	1.32	3.05	2.37	1.31	2.38	0.93
Loma Prieta	$x_{b,max}$	35.7	24.2	30.14	36.50	25.05	27.64
	$d_{s,max}$	0.20	0.19	0.20	0.21	0.19	0.19
	$\ddot{x}2_{s,max}$	2.36	2.91	2.91	2.41	2.80	2.17
Chichi	$x_{b,max}$	60.2	32.9	39.27	60.09	33.31	36.21
	$d_{s,max}$	0.34	0.23	0.24	0.34	0.23	0.21
	$\ddot{x}2_{s,max}$	3.88	3.14	3.57	3.88	2.92	2.47

4.Introduction of the Structure Under Investigation

A ten-story building in Rasht, Gilan Province, with soil type IV and X-shaped bracing was modeled in ETABS to obtain mass and stiffness matrices. The model is three-dimensional, with floors 1–3 differing from floors 4–10 to assess damper performance in an irregular structure (Figure 3). Dimensions are in meters. The structure was subjected to Chi-Chi, Kobe, Tabas, and Gazli earthquakes, with their characteristics presented in Figure 4 and Table 4.1. Responses for uncontrolled, passive, and semi-active damper-equipped structures were compared via time-history dynamic analysis. Piezoelectric friction dampers (1000 V, damping coefficient 1.1, friction coefficient 0.2) were used across four configurations, with dampers at plan corners for optimal performance (Figure 5). Floor heights are 3.4 m (first), 2.9 m (second and third), and 3.3 m (fourth to tenth). Acceleration-time records were used to solve equations in state-space form with LQR control.Figure 3: Plan view of the ten-story structure.
Three-dimensional model or plan view of the ten-story steel structure with X-shaped bracing, modeled in ETABS to evaluate damper performance in an irregular structure.

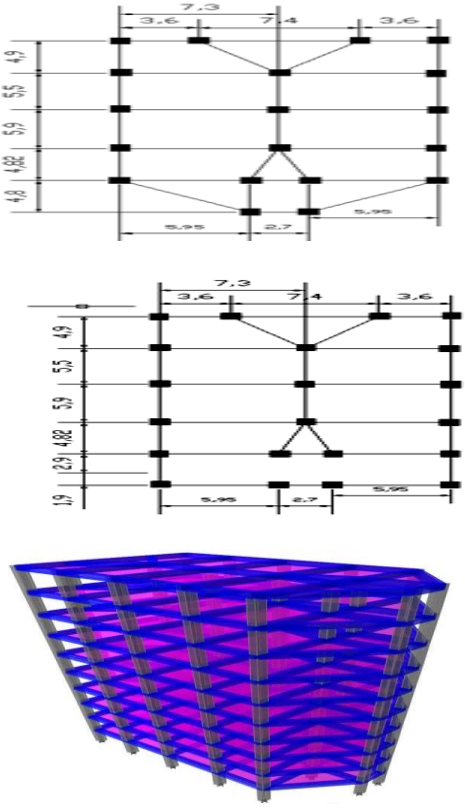

Figure 3: Plan of the desired structure; (a) one to three stories and (b) four to ten stories.

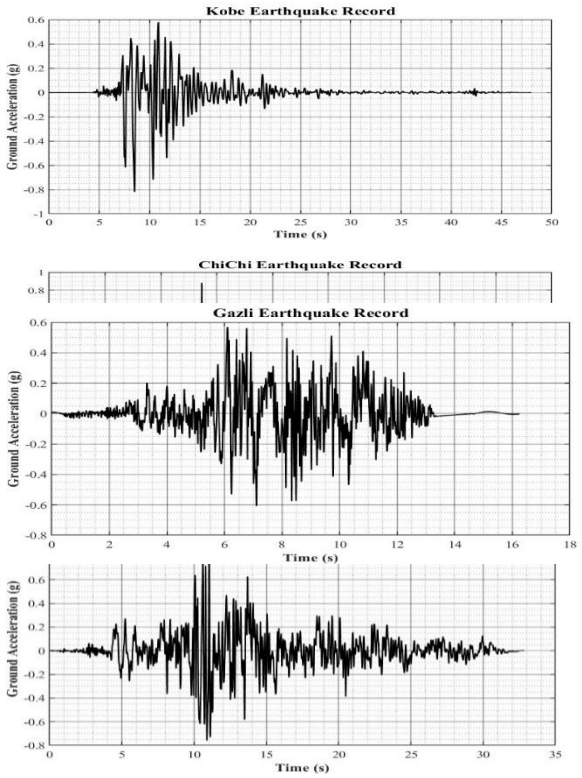

Figure 4: Characteristics of earthquake records

Table 2:
Characteristics of Earthquake Records Used in Dynamic Analysis

Earthquake	Year of Occurrence	Magnitude	Distance from Epicenter
Kobe	1995	6.8	Depth 14km (off the coast of Kobe)
Chichi	1999	7.6	8 km
Tabas	1978	7.8	15 km
Gazli	1976	7.1	10 km

A representation of the damper placement in the plan view of the structure, optimized for corner locations to enhance seismic performance, is shown in Figure 5.

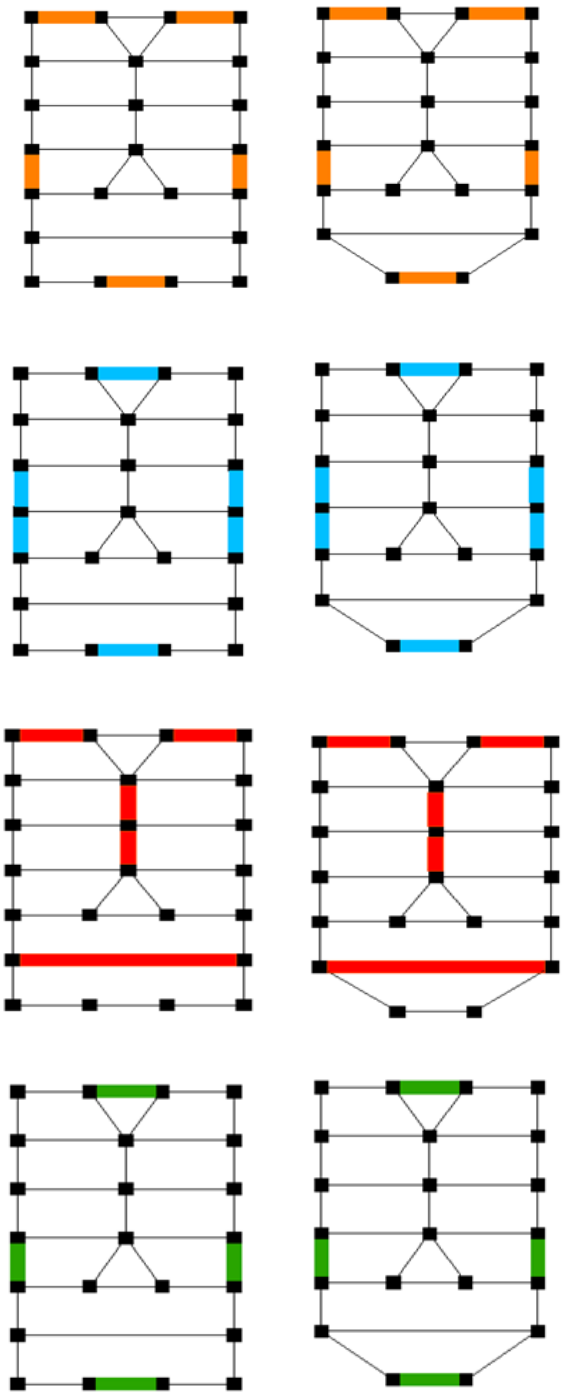

Figure 5: Damper Configuration in Plan View

5.Structural Response to Earthquakes

5-1-Response of Structures to Chi-Chi Earthquake

The ten-story structure was analyzed under the Chi-Chi earthquake in four damper configurations (Categories A–D) and three control modes (passive, semi-active, active). Semi-active mode performed best, followed by active mode

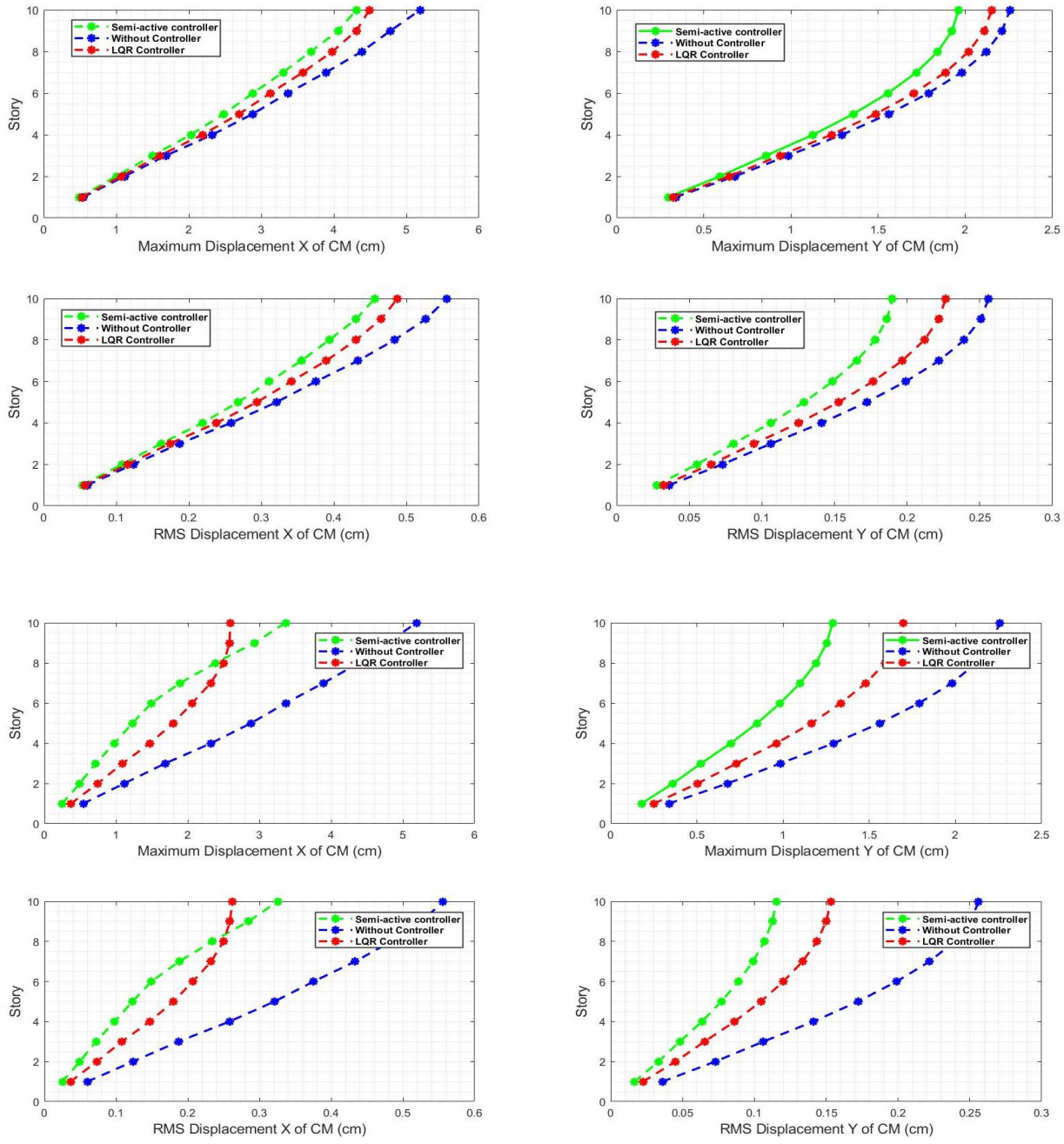

Figure 6: Maximum displacement under Chi-Chi earthquake

Table 3:
Numerical Results for Displacement and Base Shear from the Chi-Chi Earthquake (Categories A and B)

Case	Semi-active Control		Active Control		Passive Control	
	Category A	Category B	Category A	Category B	Category A	Category B
Maximum Displacement in X (cm)	2/6	2/67	2/69	54/2	5/17	5/2
Maximum Displacement in Y (cm)	1/33	1/45	1/72	72/1	2/26	2/26
Minimum Error in X Displacement (cm)	0/25	0/26	0/27	25/0	0/55	0/55
Minimum Error in Y Displacement (cm)	0/12	0/13	0/15	15/0	0/26	0/26
Maximum Acceleration in X (cm/s²)	08/7	10/8	77/7	82/7	11	11
Maximum Acceleration in Y (cm/s²)	11/44	12/23	11/44	22/12	18/35	18/48
Minimum Error in X Acceleration (cm/s²)	0/75	0/65	0/76	67/0	1/1	1/1
Minimum Error in Y Acceleration (cm/s²)	1/06	1/06	1/05	04/1	1/77	1/77
Maximum Column Displacement (cm)	2/72	2/79	2/8	66/2	5/3	5/26
Minimum Error in Column Displacement (cm)	0/28	0/28	0/31	3/0	0/62	0/61
Maximum Base Shear (kN)	472/05	440/48	667/70	246/633	881/98	5/2
Maximum Base Moment (kN•m)	7003/15	6699/29	8659/31	58/8050	14432/2	2/26

Table 4:
Numerical Results for Displacement and Base Shear from the Chi-Chi Earthquake (Categories C and D)

Case	Semi-active Control		Active Control		Passive Control	
	Category C	Category D	Category C	Category D	Category C	Category D
Maximum Displacement in X (cm)	2.96	3.22	2.71	2.74	5.17	5.16
Maximum Displacement in Y (cm)	1.46	1.21	1/78	1.70	2.28	2.29
Minimum Error in X Displacement (cm)	0.29	0.32	0.27	0.27	0.55	0.51
Minimum Error in Y Displacement (cm)	0.13	0.12	0.16	0.17	0.25	0.25
Maximum Acceleration in X (cm/s²)	8.86	8.13	8.38	8.13	11	11
Maximum Acceleration in Y (cm/s²)	12.60	11.81	12.59	11.82	18.43	18.51
Minimum Error in X Acceleration (cm/s²)	0.71	0.68	0.72	0.69	1.1	1.1
Minimum Error in Y Acceleration (cm/s²)	1.12	1.02	1.10	1.01	1.77	1.77
Maximum Column Displacement (cm)	3.05	3.31	2.82	2.86	5.29	5.32
Minimum Error in Column Displacement (cm)	0.31	0.33	0.32	0.31	0.62	0.61
Maximum Base Shear (kN)	479.745	437.71	678.233	652.048	892.744	897.742
Maximum Base Moment (kN•m)	7337.34	7924.53	8553.36	8490.57	14344.2	14339.6

5.2.Response of the Structure to the Kobe Earthquake

Analysis under the Kobe earthquake used four damper configurations and three control modes.

Plot of maximum displacement in X and Y directions for the ten-story structure under the Kobe earthquake, comparing uncontrolled, passive, and semi-active control modes.

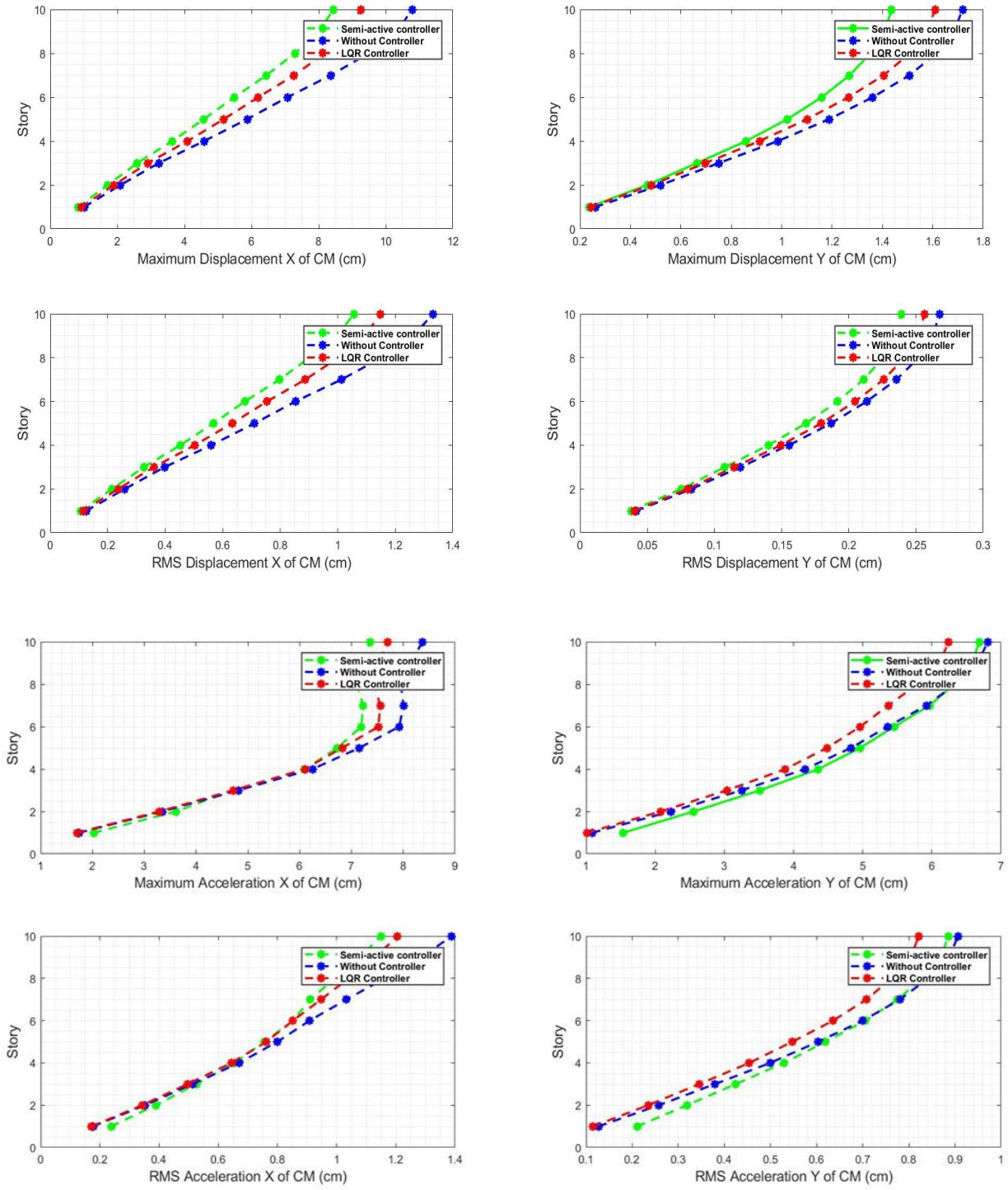

Figure 6: Maximum displacement under Chi-Chi earthquake

Table 5:
Numerical Results for Displacement and Base Shear from the Kobe Earthquake (Categories A and B)

Case	Semi-active Control		Active Control		Passive Control	
	Category A	Category B	Category A	Category B	Category A	Category B
Maximum Displacement in X (cm)	3/56	3/55	4/08	4/49	10/8	10/73
Maximum Displacement in Y (cm)	1/53	1/42	1/45	1/39	1/72	1/7
Minimum Error in X Displacement (cm)	0/48	0/48	0/54	0/58	1/33	1/32
Minimum Error in Y Displacement (cm)	0/21	0/2	0/22	0/22	0/27	0/27
Maximum Acceleration in X (cm/s²)	4/53	5/17	4/71	5/34	8/37	8/42
Maximum Acceleration in Y (cm/s²)	4/62	4/69	4/48	4/51	6/81	6/82
Minimum Error in X Acceleration (cm/s²)	0/52	0/59	0/57	0/59	1/39	1/4
Minimum Error in Y Acceleration (cm/s²)	0/63	0/63	0/59	0/59	0/9	0/92
Maximum Column Displacement (cm)	3/75	3/81	4/16	4/65	10/87	11
Minimum Error in Column Displacement (cm)	0/52	0/53	0/58	0/63	1/36	1/37
Maximum Base Shear (kN)	556/962	643/42	936/709	1022/81	1620/25	1608/29
Maximum Base Moment (kN•m)	9025/19	9869/42	12336/7	14005/6	30581/3	30434/5

Table 6:
Numerical Results for Displacement and Base Shear from the Kobe Earthquake (Categories C and D)

Case	Semi-active Control		Active Control		Passive Control	
	Category C	Category D	Category C	Category D	Category C	Category D
Maximum Displacement in X (cm)	4/2	4/54	4/6	4/54	10/74	10/84
Maximum Displacement in Y (cm)	1/5	1/4	1/45	1/44	1/72	1/72
Minimum Error in X Displacement (cm)	0/57	0/6	0/6	0/58	1/34	1/32
Minimum Error in Y Displacement (cm)	0/2	0/18	0/22	0/22	0/27	0/27
Maximum Acceleration in X (cm/s²)	4/9	4/82	5	5	8/38	8/37
Maximum Acceleration in Y (cm/s²)	4/88	4/54	4/61	4/43	6/81	6/85
Minimum Error in X Acceleration (cm/s²)	0/57	0/57	0/62	0/61	1/39	1/39
Minimum Error in Y Acceleration (cm/s²)	0/66	0/62	0/61	0/57	0/9	0/9
Maximum Column Displacement (cm)	4/36	4/71	4/62	4/56	10/88	10/87
Minimum Error in Column Displacement (cm)	0/59	0/64	0/64	0/64	1/36	1/37
Maximum Base Shear (kN)	609/191	569/391	1011/06	982/336	1597/82	1599/95
Maximum Base Moment (kN•m)	10359/3	10470	14049/2	13397	30454/4	30407/5

5.3.Response of the Structure to the Tabas Earthquake

Analysis under the Tabas earthquake followed the same approach.

.

Plot of maximum displacement in X and Y directions for the ten-story structure under the Tabas earthquake, comparing uncontrolled, passive, and semi-active control modes

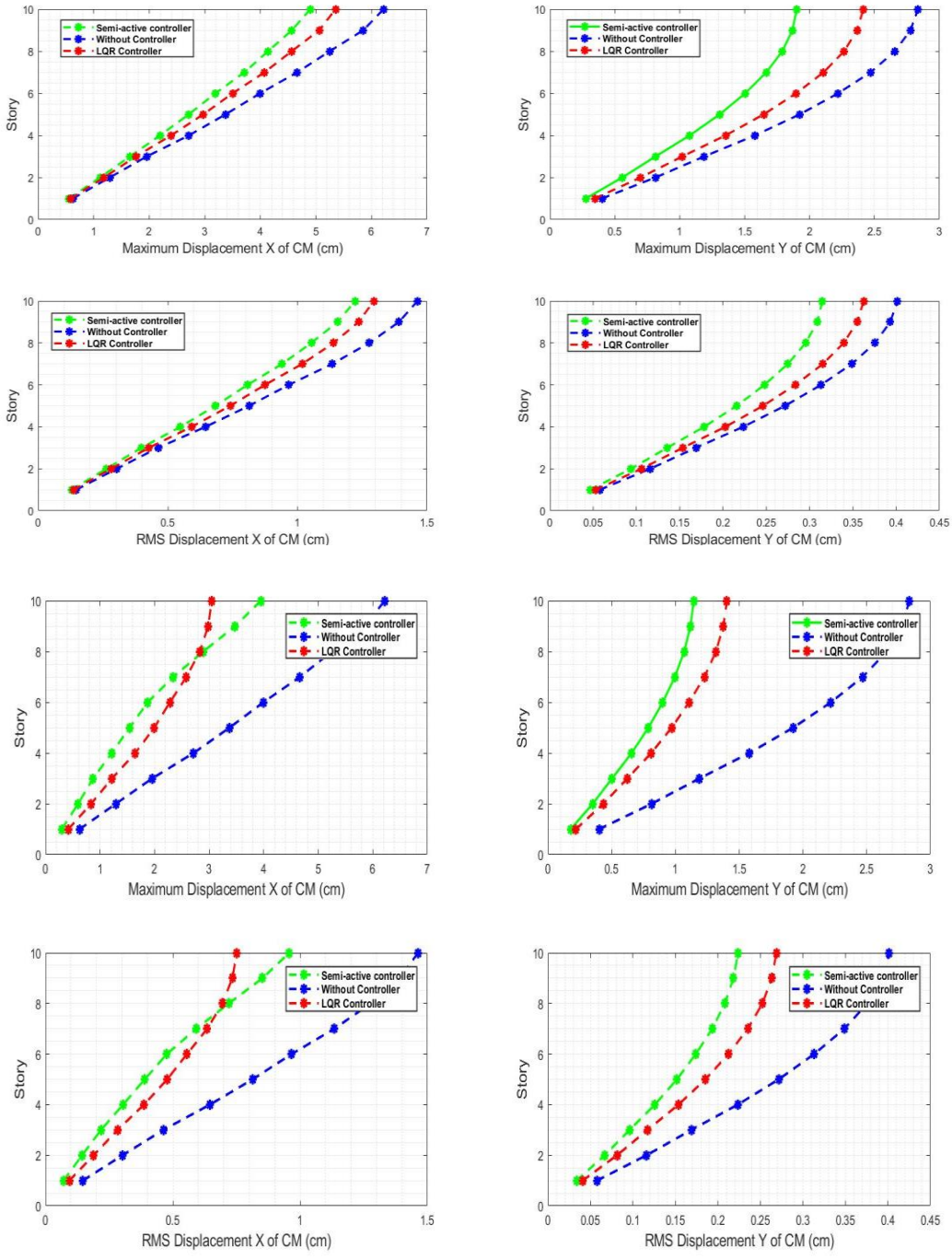

Figure 8: Maximum displacement under Tabas earthquake

Table 7:
Numerical Results for Displacement and Base Shear from the Tabas Earthquake (Categories A and B)

Case	Semi-active Control		Active Control		Passive Control	
	Category A	Category B	Category A	Category B	Category A	Category B
Maximum Displacement in X (cm)	3/12	3/08	3/18	2/95	6/25	6/19
Maximum Displacement in Y (cm)	1/17	1/26	1/42	1/42	2/85	2/85
Minimum Error in X Displacement (cm)	0/75	0/76	0/77	0/73	1/46	1/47
Minimum Error in Y Displacement (cm)	0/23	0/24	0/27	0/27	0/4	0/4
Maximum Acceleration in X (cm/s²)	10/53	9/26	10/79	9/54	14/31	14/42
Maximum Acceleration in Y (cm/s²)	15/04	15/14	15/04	15/14	26/63	26/59
Minimum Error in X Acceleration (cm/s²)	1/25	1/09	1/27	1/12	1/79	1/79
Minimum Error in Y Acceleration (cm/s²)	1/74	1/75	1/72	1/73	2/78	2/79
Maximum Column Displacement (cm)	3/21	3/22	3/25	3/07	6/34	6/32
Minimum Error in Column Displacement (cm)	0/78	0/79	0/83	0/78	1/53	1/53
Maximum Base Shear (kN)	509/554	498/432	726/115	694/006	1000	993/691
Maximum Base Moment (kN•m)	8492/17	7792/28	9893/01	9092/17	16707/7	16602/7

Table 8:
Numerical Results for Displacement and Base Shear from the Tabas Earthquake (Categories C and D)

Case	Semi-active Control		Active Control		Passive Control	
	Category C	Category D	Category C	Category D	Category C	Category D
Maximum Displacement in X (cm)	3/45	3/72	3/21	3/18	6/23	6/17
Maximum Displacement in Y (cm)	1/25	1/08	1/52	1/36	2/85	2/8
Minimum Error in X Displacement (cm)	0/84	0/88	0/79	0/78	1/47	1/46
Minimum Error in Y Displacement (cm)	0/24	0/21	0/28	0/26	0/4	0/4
Maximum Acceleration in X (cm/s²)	9/85	9/3	10/02	9/61	14/32	14/34
Maximum Acceleration in Y (cm/s²)	15/67	14/53	15/67	14/53	26/55	26/55
Minimum Error in X Acceleration (cm/s²)	1/19	1/13	1/21	1/14	1/79	1/79
Minimum Error in Y Acceleration (cm/s²)	1/84	1/71	1/82	1/69	2/79	2/79
Maximum Column Displacement (cm)	3/57	3/77	3/26	3/25	6/33	6/34
Minimum Error in Column Displacement (cm)	0/86	0/92	0/83	0/83	1/52	1/53
Maximum Base Shear (kN)	517/282	500	722/714	711/538	991/613	1000
Maximum Base Moment (kN•m)	8770/21	9254/61	9928/92	9788/73	16700	16456/4

5.4.Response of the Structure to the Gazli Earthquake

Analysis under the Gazli earthquake used the same methodology.Plot of maximum displacement in X and Y directions for the ten-story structure under the Gazli earthquake, comparing uncontrolled, passive, and semi-active control modes

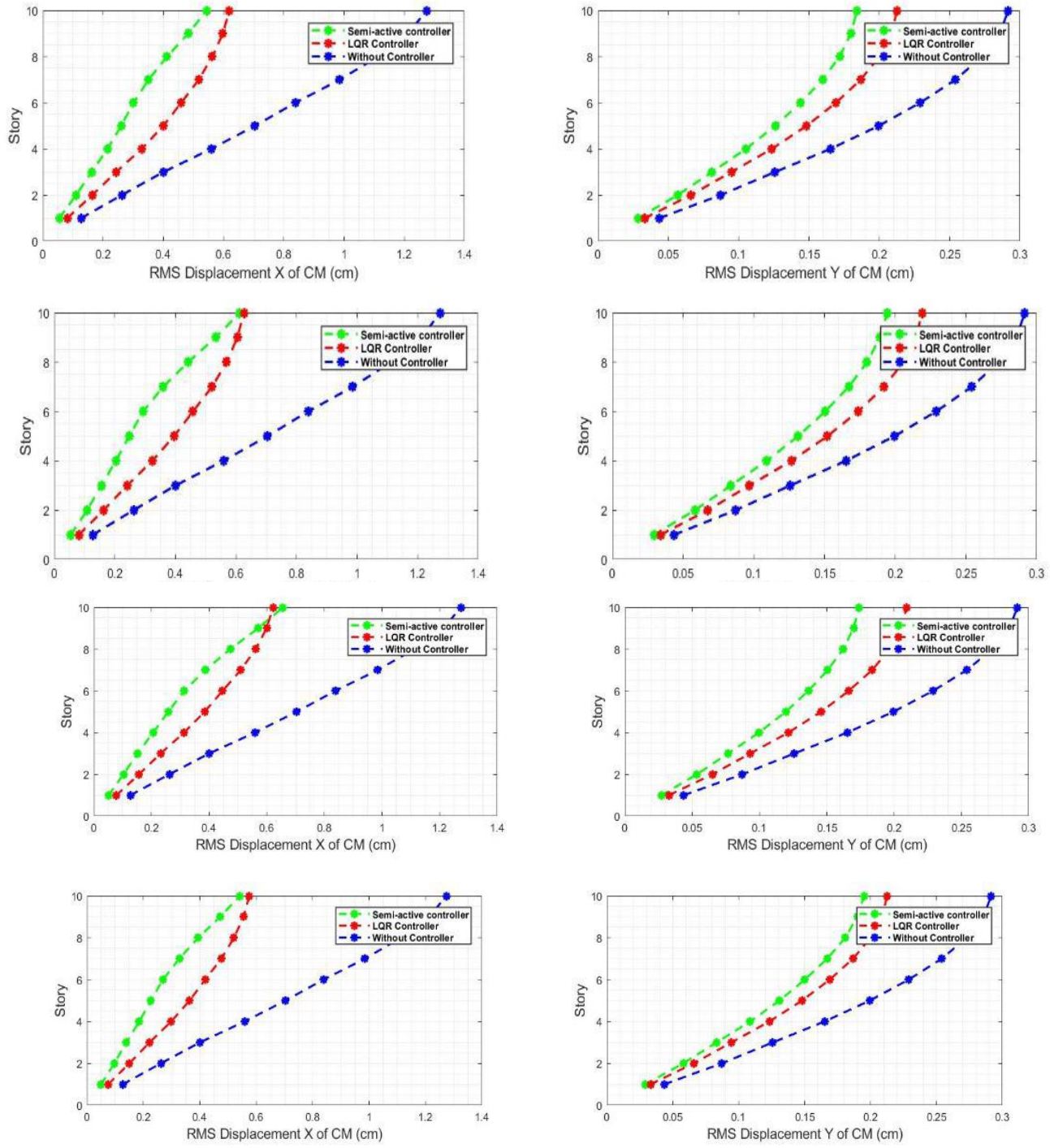

Figure 9: Maximum displacement under Gazli earthquake

Case	Semi-active Control		Active Control		Passive Control	
	Category A	Category B	Category A	Category B	Category A	Category B
Maximum Displacement in X (cm)	1/79	1/79	1/94	2/09	4/41	4/39
Maximum Displacement in Y (cm)	0/89	0/83	1	1	1/4	1/4
Minimum Error in X Displacement (cm)	0/54	0/55	0/57	0/62	1/27	1/27
Minimum Error in Y Displacement (cm)	0/19	0/18	0/21	0/21	0/29	0/29
Maximum Acceleration in X (cm/s²)	7/04	6/96	7/04	6/88	9/71	9/5
Maximum Acceleration in Y (cm/s²)	8/17	8/34	8/08	8/22	11/37	11/28
Minimum Error in X Acceleration (cm/s²)	1/22	1/18	1/19	1/17	1/57	1/57
Minimum Error in Y Acceleration (cm/s²)	1/51	1/5	1/51	1/5	2/25	2/24
Maximum Column Displacement (cm)	1/89	1/86	2/05	2/16	4/52	4/5
Minimum Error in Column Displacement (cm)	0/58	0/57	0/63	0/65	1/32	1/32
Maximum Base Shear (kN)	268/354	292/386	420/253	446/639	708/861	700/83
Maximum Base Moment (kN•m)	4275	4292/9	5587/5	5899/62	11775	11682/2

Table 10:
Numerical Results for Displacement and Base Shear from the Gazli Earthquake (Categories C and D

Case	Semi-active Control		Active Control		Passive Control	
	Category C	Category D	Category C	Category D	Category C	Category D
Maximum Displacement in X (cm)	2/03	2/22	2/12	2/12	4/39	4/45
Maximum Displacement in Y (cm)	0/88	0/77	1/02	0/98	1/41	1/41
Minimum Error in X Displacement (cm)	0/6	0/66	0/62	0/62	1/27	1/28
Minimum Error in Y Displacement (cm)	0/19	0/17	0/21	0/21	0/29	0/29
Maximum Acceleration in X (cm/s²)	7/46	7	7/36	6/88	9/56	9/54
Maximum Acceleration in Y (cm/s²)	8/31	8/05	8/22	8/05	11/33	11/33
Minimum Error in X Acceleration (cm/s²)	1/26	1/18	1/25	1/16	1/57	1/57
Minimum Error in Y Acceleration (cm/s²)	1/59	1/49	1/59	1/49	2/26	2/25
Maximum Column Displacement (cm)	1/1	2/24	1/18	2/18	4/49	4/49
Minimum Error in Column Displacement (cm)	0/64	0/67	0/67	0/66	1/31	1/31
Maximum Base Shear (kN)	301/558	261/978	451/09	426/099	710/28	704/202
Maximum Base Moment (kN•m)	4762/5	4990/48	4887/5	5752/38	11775	11733/3

6-Discussion and Analysis of Results

6-1- Comparison of Results from Earthquakes in Categories A and B

Category A dampers during Chi-Chi, Kobe, Tabas, and Gazli earthquakes yielded X-direction displacements in semi-active mode of 2.6, 3.56, 3.12, and 1.79 cm; active mode: 2.69, 4.08, 3.18, and 1.94 cm; passive mode: 5.17, 10.8, 6.25, and 4.41 cm. Semi-active mode consistently showed lower displacements, with base shear in active and passive modes increasing by 41.4% and 86.84% for Chi-Chi. For Kobe, active and semi-active modes reduced displacement by 62.2% and 67% compared to passive mode.

Category B dampers showed similar trends, with X-direction displacements in semi-active mode of 2.67, 3.55, 3.08, and 1.79 cm; active mode: 2.54, 4.49, 2.95, and 2.09 cm; passive mode: 5.2, 10.73, 6.19, and 4.39 cm. Base shear for Chi-Chi in active and passive modes increased by 43.7% and 101.74%.

6-2- Comparison of Results from Earthquakes in Categories C and D

Category C dampers showed X-direction displacements in semi-active mode of 2.96, 4.2, 3.45, and 2.03 cm; active mode: 2.71, 4.6, 3.18, and 2.12 cm; passive mode: 5.17, 10.74, 6.23, and 4.39 cm. Base shear for Chi-Chi in active and passive modes increased by 41.4% and 86.6%.

Category D dampers showed X-direction displacements in semi-active mode of 3.22, 4.54, 3.72, and 2.22 cm; active mode: 2.74, 4.54, 2.18, and 2.12 cm; passive mode: 5.16, 10.86, 6.17, and 4.45 cm. Base shear for Chi-Chi in active and passive modes increased by 48.9% and 105.09%.

Category A (six dampers) performed best, followed by B (five), C (four), and D. For Chi-Chi, Category A's displacement was 0.07, 0.36, and 0.62 cm less than B, C, and D, respectively, corresponding to 2.6%, 12.16%, and 19.25% better performance.

7.Conclusion

- Semi-active friction dampers significantly reduce structural displacement.
- Placing dampers at building plan corners yields optimal performance.
- Semi-active mode outperforms active and passive modes.
- Passive friction dampers reduce structural responses acceptably.
- Semi-active dampers are more effective than passive and active dampers in improving seismic behavior.
- The impact of semi-active dampers varies across earthquakes, influenced by structural response type.
- Selecting an appropriate design earthquake is critical for effective semi-active systems.
- Maximum base shear and moment are lowest in semi-active mode. For Chi-Chi, Category A base shear increased by 41.4% (active) and 86.84% (passive); Category B by 43.7% and 101.74%; Category C by 41.4% and 86.6%; Category D by 48.9% and 105.09%.
- Category A (six dampers) is optimal, followed by B (five), C (four), and D.

References

[1] Cheng, F.Y., Jiang, H., Lou, K. (2008).Smart Structures: Innovative Systems for Seismic Response Control.CRC Press, Boca Raton, FL.

[2] Fisco, N.R., Adeli, H. (2011).Active and semi-active control of structures.Scientia Iranica, 18(3), 275–284. https://doi.org/10.1016/j.scient.2011.05.034

[3] Ghanadi Asl, A., Abbaszadeh, Z., Shirkhani, A., Kamrani Moghadam, P. (2022).Seismic performance of an out-of-plane braced frame system with optimized steel shear panel and rotational friction damper at various seismic levels.Journal of Structural Engineering and Construction, 9(9), 23–42.

[4] Kobori, T., Minai, R. (1960).Analytical study on active seismic response control.Transactions of the Architectural Institute of Japan, 66, 257–260.

[5] Liao, W.I., Mualla, I.H., Loh, C.H. (2004).Shaking table test of a friction-damped frame structure.The Structural Design of Tall and Special Buildings, 13(1), 45–54. https://doi.org/10.1002/tal.231

[6] Lu, L.Y., Lin, T.K., Jheng, R.J., Wu, H.H. (2018).Theoretical and experimental investigation of position-controlled semi-active friction damper for seismic structures.Journal of Sound and Vibration, 412, 184–206. https://doi.org/10.1016/j.jsv.2017.09.029

[7] Mualla, I.H. (2000).Experimental evaluation of a new friction damper device.Proceedings of the 12th World Conference on Earthquake Engineering (12WCEE),Paper No. 1048.

[8] Nazari Monfared, H., Zohraei, M. (2016).Seismic control of multi-story buildings using active tendons considering soil–structure interaction.
Journal of Earthquake Engineering, 20(5), 781–799. https://doi.org/10.1080/13632469.2015.1104750

[9] Ng, C.L., Xu, Y.L. (2007).Semi-active control of a building complex with variable friction dampers.Engineering Structures, 29(6), 1209–1225. https://doi.org/10.1016/j.engstruct.2006.08.018

[10] Ozbulut, O.E., Bitaraf, M., Hurlebaus, S. (2011).Adaptive control of base-isolated structures against near-field earthquakes using variable friction dampers.Engineering Structures, 33(12), 3143–3154. https://doi.org/10.1016/j.engstruct.2011.08.022

[11] Pall, A.S., Marsh, C. (1982).Response of friction-damped braced frames.Journal of the Structural Division, ASCE, 108(6), 1313–1323.

[12] Shirkhani, A., Azar, B.F., Basim, M.C. (2021).Seismic loss assessment of steel structures equipped with rotational friction dampers subjected to intensifying dynamic excitations.Engineering Structures, 238, 112233. https://doi.org/10.1016/j.engstruct.2021.112233

[13] Shirkhani, A., Mualla, I.H., Shabakhty, N., Mousavi, S.R. (2015).Behavior of steel frames with rotational friction dampers using the endurance time method.Journal of Constructional Steel Research, 107, 211–222. https://doi.org/10.1016/j.jcsr.2015.01.016
[14] Soong, T.T. (1990).Active Structural Control: Theory and Practice.Longman Scientific & Technical, Wiley.
[15] Yao, J.T.P. (1972).Concept of structural control.Journal of the Structural Division, ASCE, 98(7), 1567–1574.
[16] Zamani, A., Tavakoli, S., Etedali, S. (2017).Fractional-order PID control design for semi-active control of smart base-isolated structures using a multi-objective cuckoo search approach.ISA Transactions, 67, 222–232. https://doi.org/10.1016/j.isatra.2017.01.012